



OPEN Curcumin liposomes alleviate senescence of bone marrow mesenchymal stem cells by activating mitophagy

Wei Yao Li^{1,3}, Yixin Huang^{1,3}, Lei Fan¹, Dekyi Yangzom¹, Kun Zhang¹, Lihong Shen¹, Suizhong Cao¹, Congwei Gu²✉ & Shumin Yu¹✉

The senescence of mesenchymal stem cells (MSCs) is closely related to aging and degenerative diseases. Curcumin exhibits antioxidant and anti-inflammatory effects and has been extensively used in anti-cancer and anti-aging applications. Studies have shown that curcumin can promote osteogenic differentiation, autophagy and proliferation of MSCs. Liposome, as a nano-carrier, provides a feasible strategy for improving the bioavailability and controlled-release profile of curcumin. This study aimed to evaluate the effects of curcumin liposomes (Cur-Lip) on the senescence of rat bone marrow mesenchymal stem cells (rBMSCs). Based on network pharmacology, we predicted the targets and mechanisms of curcumin on senescence of MSC. 23 key targets of Cur were associated with MSC senescence were screened out and mitophagy signaling was significantly enriched. Cur-Lip treatment alleviated senescence of D-galactose (D-gal)-induced rBMSCs, protected mitochondrial function, and activated mitophagy, which may be related to mitochondrial fission. Inhibition of mitophagy attenuated the protective effects of Cur-lip on mitochondrial function and senescence of rBMSCs. Our findings suggested that Cur-Lip could alleviate senescence of rBMSC and improve mitochondrial function by activating mitophagy.

Keywords Curcumin liposomes, rBMSCs, Network pharmacology, Mitophagy, Senescence

Mesenchymal stem cells (MSCs) are pluripotent stromal cells derived from mesoderm and are distributed in almost all tissues and organs of the body such as bone marrow, fat, and umbilical cord. MSCs are related to tissue regeneration and repair, and have great potential in the treatment of degenerative diseases^{1,2}. However, aging is accompanied by the depletion of MSCs, contributing to the development of age-related diseases³. The strategy proposed in current study was to prevent aging by retarding the senescence of MSCs through the use of dietary supplements and natural bioactive products⁴.

It is generally believed that the senescence of MSCs is mainly caused by the accumulation of large amounts of reactive oxygen species (ROS)⁵. Mitochondrial dysfunction leads to oxidative stress, thereby triggering the senescence of MSCs⁶. Mitochondrial quality control including mitochondrial biogenesis, mitochondrial dynamics, and mitophagy plays an important role in maintaining mitochondrial integrity and function, and plays pivotal roles in metabolic and aging-related diseases^{7,8}. Mitophagy, as a quality control process of mitochondria, removes damaged mitochondria in cells through the lysosomes for degradation and maintains mitochondrial homeostasis⁹. Therefore, regulating the activity of mitophagy in MSCs is expected to be an effective means to improve their oxidative stress tolerance and thereby delay premature senescence^{10,11}.

Curcumin (Cur) is a natural active substance extracted from Zingiberaceae plants, with various biological activities such as antioxidant, anti-inflammatory, and anti-tumor, making it a promising anti-aging compound for the prevention and treatment of degenerative diseases^{12,13}. In previous studies, Cur promote autophagy and proliferation of MSCs¹⁴. Cur can also regulate mitochondrial biogenesis and mitophagy, maintaining mitochondrial homeostasis, thereby ameliorating conditions such as osteoarthritis and renal injury^{15–17}. However, the therapeutic efficacy of Cur is constrained due to its low aqueous solubility and stability. To improve the stability and bioavailability of Cur, nanoparticle delivery can be utilized¹⁸. Liposomes have been developed as nanocarriers with easy preparation and high loading efficiency. Delivering Cur through it can improve aqueous

¹Department of Clinical Veterinary Medicine, College of Veterinary Medicine, Sichuan Agricultural University, Chengdu 611130, China. ²Laboratory Animal Centre, Southwest Medical University, Luzhou 646000, China. ³Wei Yao Li and Yixin Huang contributed equally to this work. ✉email: gcw081543@163.com; yayushumin@sicau.edu.cn

solubility and control the release rate in vivo, improving the stability and bioavailability of Cur^{19,20}. It has been shown Cur enhance MSC activity, but the effects of different doses, treatment length and forms of Cur on MSCs may not be consistent²¹. Moreover, whether Cur can improve oxidative stress damage and delay the senescence of MSCs by regulating mitophagy has not yet been confirmed.

Network pharmacology has become a prominent research method in the field of ethnic medicine. This approach enables the elucidation of molecular-level interactions between disease, targets, and drugs, helping to understand the mechanism of drugs more systematically and comprehensively^{22,23}. In this study, we used network pharmacology to predict the potential targets and molecular mechanism of Cur in the senescence of MSCs, and identify the protective effects of Cur-Lip on the senescence of rBMSCs induced by D-galactose (D-gal).

Materials and methods

Network pharmacologic analysis

Potential targets of Cur were screened out based on Pharmmapper (<http://www.lilab-ecust.cn/pharmmapper>), Swiss Target (<http://www.swisstargetprediction.ch/>) and Herb (<http://herb.ac.cn/>) databases, duplicates were removed. Genes that related to senescent MSCs were acquired using the Genecard database. Compared senescent MSCs -related genes with predicted Cur targets, drew a Venn diagram (<https://bioinfogp.cnb.csic.es/tools/venny/>), and obtained co-targets, which were considered as potential targets for Cur against senescent MSCs. Then imported the co-targets into String (<https://string-db.org/>) and constructed the protein-protein interaction (PPI) network diagram. The data of PPI was imported into Cytoscape 3.9.1. Nodes with degree centrality (DC), between centrality (BC), eigenvector centrality (EC), and closeness centrality (CC) greater than median value were regarded as key targets, and were screened out by using CytoNCA. The key targets were subjected to DAVID (<https://david.ncifcrf.gov/>) for further analysis. The species sources of the above data were limited to “*Homo sapiens*”.

Obtained the SDF format files of Cur from PubChem, used AutoDock software (Version 1.5.7) to configure the torque and generate the pdbqt file. The structure of the target protein was retrieved from the PDB (<https://david.ncifcrf.gov/>). PyMOL (Version 4.6.0) and AutoDock software were used to prepare the protein. AutoDock software was used to perform docking simulations and calculate binding energy during molecular docking. Binding energy reflects the likelihood of binding between the receptor and the ligand. The lower the binding energy, the higher the affinity between the receptor and the ligand. The results of molecular docking were visualized in PyMOL software.

Experimental validation

Isolation, culture, and identification of rBMSCs

All experiments were performed in accordance with relevant guidelines and regulations. All methods were reported in accordance with ARRIVE guidelines, and approved by the Institutional Animal Care and Use Committee of Southwest Medical University (Approval No. swmu20230085). At the end of the study, euthanasia was performed by injecting an overdose of pentobarbital sodium, followed by cervical dislocation.

Three to four-week-old Sprague-Dawley (SD) rats were provided by the Experimental Animal Centre of Southwest Medical University (Luzhou, China). The rats were cervical dislocated, separated femur of the rats and removed the attached tissue, irrigate the marrow cavity with a syringe drawing the medium, the rinsed culture medium was collected and centrifuged at 1500r/min for 4 min. After suspension, the cells were inoculated in T25 culture bottles and cultured in a 5%CO₂ incubator at 37 °C. rBMSCs were isolated and cultured according to the reference²⁴. Cells used in this study were from the passages 3 to 5. The cultured cells were confirmed to be rBMSCs through surface antigens detection, and osteogenic and adipogenic-induced differentiation experiments.

Detection of rBMSCs senescence

There were six groups in this study: (1) control group, (2) D-gal (32 mg/mL, Beyotime, China) group, (3) D-gal (32 mg/mL) + Cur-Lip low-dose (5 μmol/L, ruixi Bio-Technology Co., Ltd) group, (4) D-gal (32 mg/mL) + Cur-Lip high-dose (10 μmol/L) group, (5) D-gal (32 mg/mL) + Mdivi-1 (5 μmol/L, MCE, USA) + Cur-Lip (10 μmol/L) group, (6) D-gal (32 mg/mL) + Rapamycin (200 nmol/L, MCE, USA) group, the treatment time of each group was 48 h.

rBMSCs were processed according to groups and stained using senescence-associated beta-galactosidase (SA-β-gal) staining kits (Beyotime, China). Senescence cells would appear blue and the number of blue cells per 100 cells were counted.

Ki67 immunofluorescence staining was used to detect cell proliferation. Treated rBMSCs were fixed with 4% paraformaldehyde for 30 min at room temperature and permeabilized with 0.1% Triton X-100 for 20 min. After washing with PBS, cells were blocked with 3% BSA at room temperature for 30 min. Cells were incubated with antibody Anti-Ki67 (1:250, Abcam, UK) overnight at 4 °C, and then incubated with anti-rabbit secondary antibody (1:1000, CST, USA) at room temperature for 60 min. Finally, the nuclei were stained with DAPI for 10 min at room temperature and detected by fluorescence inverted microscope.

Colony formation assay was used to detect cell viability and proliferation. rBMSCs were inoculated in 6-well plates (400 cells/well). After 14 days, rBMSCs were fixed with 4% paraformaldehyde for 15 min, then stained with crystal violet solution for 10 min.

Detection of mitochondrial function and mitophagy

Mitochondrial membrane potential (mtΔψ_m) was detected following the JC-1 dye protocol (Beyotime), and observed under a fluorescence microscope. The level of mtΔψ_m was analyzed by calculating the green fluorescent/

red fluorescent intensity ratio. MitoSOX Red staining (YEASEN, China) was used to detect mitochondrial ROS. MitoSOX Red was diluted to a final concentration of 5 $\mu\text{mol/L}$, incubated the cells at 37 °C without exposure to light for 10 min.

The level of mitophagy was evaluated using co-localization staining of mitochondria and lysosomes. The cell was incubated at 37 °C in MitoTracker Red dyeing solution (200 nM, Yeasen, China) and the Lyso-Tracker Green (60 nM, Beyotime, China) for 30 min. The nucleus was stained with DAPI.

Cell samples of each group were collected and RNA was extracted by commercial kits (TIANGEN, China). One μg of RNA of each sample was used as the template for reverse transcription. The fluorescence quantitative PCR procedure was executed according to the instructions of the TB Green kit (Takara, Japan), and the mRNA relative expressions of the *PCG-1 α* , *Drp1*, *Mfn1*, *Mfn2*, and *OPA1* genes were analyzed by the $2^{-\Delta\Delta\text{Ct}}$ method. The detailed information on primers is shown in Supplementary file S1.

Western blotting

After extracting the total protein of each group and determining concentration, thirty μg of protein was subjected to 12.5% SDS-PAGE, transferred to polyvinylidene fluoride membranes, and then blocked in 5% skim milk for 1 h. After washing with phosphate buffered saline with tween (PBST), the membrane was incubated with p21 (1:1000, Abcam, UK), p16INK4a (1:1000, Abcam, UK), p53 (1:1000, CST, USA), LC3B (1:1000, CST, USA), p62 (1:1000, CST, USA), PINK1 (1:1000, Abcam, UK), Parkin (1:1000, Abcam, UK) and mouse anti- β -actin (1:1000, CST, USA) overnight at 4 °C. Put the membrane into the secondary antibody (1:10000, CST, USA), and incubated at room temperature for 1 h. The relative protein expressions were shown as the ratio between its intensity to that of β -actin.

Statistical analysis

GraphPad Prism 9.0 was used for statistical graphing. The results of WB were analyzed using Image J. One-way analysis of variance (ANOVA) was used for multiple samples, $P < 0.05$ indicated significant differences.

Results

Predicted mechanisms of Cur in delaying the senescence of MSCs

In total, 483 potential target genes of Cur and 2047 senescent MSCs related genes were screened out from the online databases. There were 196 co-targets between Cur and senescence of MSCs (Fig. 1A). The PPI network of 196 genes was constructed using STRING, and 23 key targets were selected by CytoCNA, including TP53, AKT1, STAT3, CTNBN1, TNF and SRC. (Fig. 1B, Supplementary file S2).

A total of 432 GO entries were finally enriched, including 27 cellular components (CC), 347 biological processes (BP), and 58 molecular functions (MF). GO entries for each category were analysed and partially terms shown in Fig. 1C ($p < 0.01$). KEGG results showed 157 signaling pathways were obtained, and the pathways related to cell proliferation and senescence were significantly enriched ($p < 0.01$), involved in cancer pathway, FOXO signaling pathway, HIF-1 signaling pathway and mitophagy (Fig. 1D, $p < 0.01$, Supplementary file S2). Interestingly, the targets TP53, MAPK8, SRC, HRAS, and HIF1A of Cur-Lip on senescent MSCs is closely related to mitophagy (Fig. 1E).

Molecular docking analysis showed that Cur can interact with crystal structures of Tp53, MAPK8, HRAS, SRC, and HIF1 α , and the overall conformation can be observed in Fig. 2. The hydrogen bond formed between the Cur and the amino acid residue Ser1548 of Tp53 (Fig. 2A). Cur forms hydrogen bonds with His82, LYS78, and LYS166 of MAPK8 (Fig. 2B). The formation of hydrogen bonds between Cur and specific amino acid residues of HARS, namely ASP119 and VAL29 (Fig. 2C). Cur establishes hydrogen bonds with ASP493, ARG480, and ARG500 of SRC (Fig. 2D). Likewise, Cur establishes hydrogen bonds with PRO229, GLN241, and GLU225 of HIF1 α (Fig. 2E). Binding energy less than zero suggests that the ligand and receptor have the propensity to spontaneously bind, with lower values indicating a higher degree of binding affinity. The binding energy of Cur with Tp53, MAPK8, HRAS, SRC, and HIF1 α were -4.3 kcal/mol, -8.44 kcal/mol, -9.33 kcal/mol, -6.52 kcal/mol and -5.66 kcal/mol, respectively. In summary, Cur can bind to mitophagy-related protein targets, thereby directly regulating the mitophagy pathway.

Cur-Lip attenuated senescence of rBMSCs

In this study, rBMSCs was isolated and identified (Supplementary file S3). The SA- β -gal and the expression of p16, p21, and p53 proteins were assayed to evaluate the protective effect of Cur-Lip on senescence of MSCs (Fig. 3). D-gal treatment increased SA- β -gal positive cells (Fig. 3A, $p < 0.01$). Furthermore, western blotting results revealed that age-associated proteins p16, p21, and p53 increased significantly in the D-gal group compared to the control group (Fig. 3B, $p < 0.05$, $p < 0.01$). Different Cur-Lip treatments (5 $\mu\text{mol/L}$ and 10 $\mu\text{mol/L}$) exhibited a significant decrease of SA- β -gal positive cells (Fig. 3A, $p < 0.01$), the expressions of p16, p21 and p53 proteins in rBMSCs were downregulated (Fig. 3B, $p < 0.05$, $p < 0.01$). These results suggested that Cur-Lip could prevent the senescence of rBMSCs induced by D-gal, but Cur-Lip at a concentration of 20 $\mu\text{mol/L}$ or above showed no significant beneficial effect (Supplementary file S4).

Cur-Lip improved cell proliferation in senescent rBMSC

The CFU and Ki67 staining were assayed to evaluate the cell proliferation capacity of rBMSCs (Fig. 4). D-gal treatment reduced colony formation (Fig. 4A) and decreased Ki67-positive cells (Fig. 4B, $p < 0.01$) compared with the control group. 5 $\mu\text{mol/L}$ and 10 $\mu\text{mol/L}$ Cur-Lip treatment improved the rBMSCs clone formation rate (Fig. 4A) and increased Ki67-positive cells (Fig. 4B, $p < 0.01$). These results suggested that Cur-Lip could improve cell proliferation in D-gal induced senescent rBMSCs.

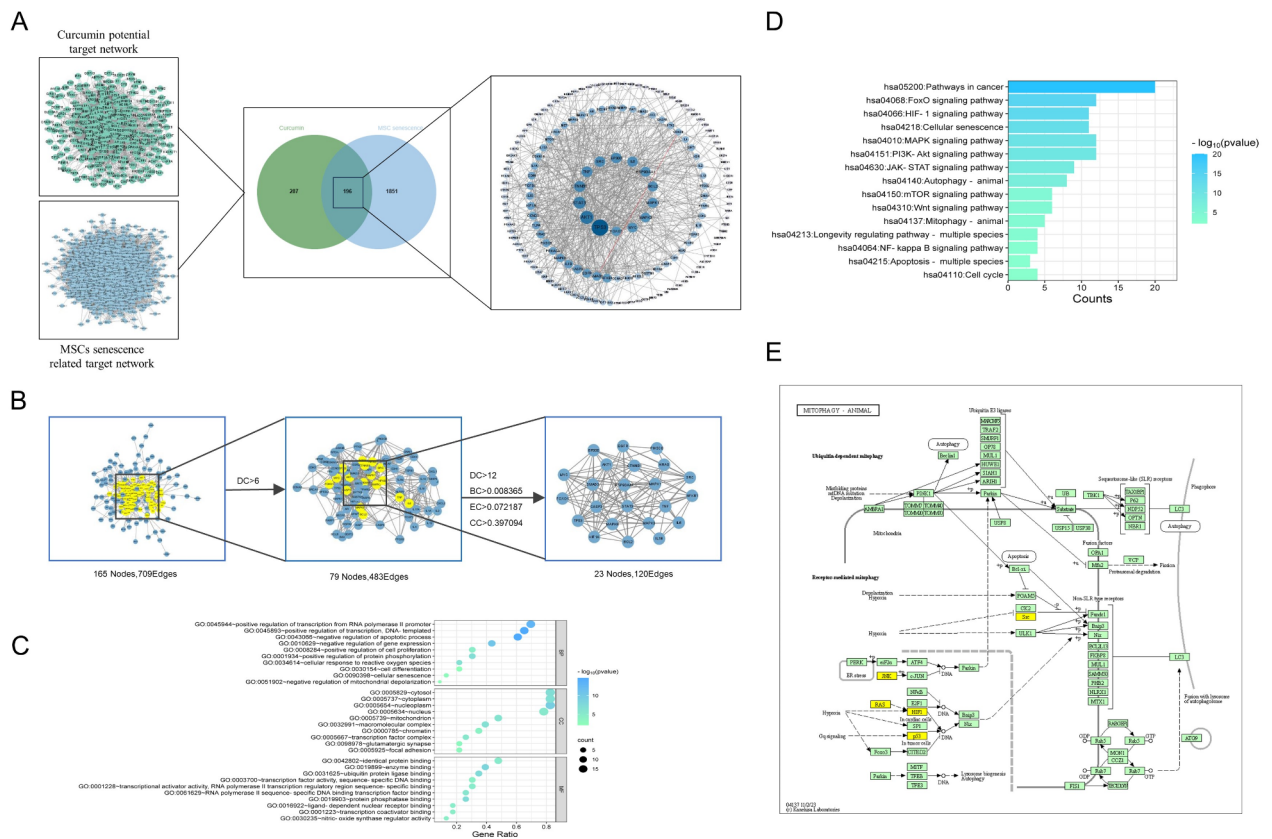


Fig. 1. Network pharmacology analysis predicted the mechanisms of the Cur effect on the senescence of MSCs. **(A)** The screening process for Cur-senescent MSCs co-targets. **(B)** Topology analysis and key target screening. **(C)** GO enrichment analysis of BP, CC, and MF. **(D)** KEGG enrichment analysis of anti-MSC senescence core target of Cur. **(E)** Mitophagy pathway²⁵.

Cur-Lip protected mitochondrial function in rBMSCs

To assess the effect of Cur-Lip against mitochondrial dysfunction in rBMSCs, mtROS, mtROS and mt $\Delta\psi$ m were analysed (Fig. 5). Compared with the control group, the D-gal group exhibited an increase in intracellular mtROS (Fig. 5A, $p < 0.01$) and lower mt $\Delta\psi$ m (Fig. 5B, $p < 0.01$). 5 μ mol/L and 10 μ mol/L Cur-Lip treatment reduced mtROS (Fig. 5A, $p < 0.01$) and increased mt $\Delta\psi$ m (Fig. 5B, $p < 0.05$, $p < 0.01$) but not restored to the normal levels.

Cur-Lip promoted mitochondrial quality control in rBMSCs

To analyze the effect of Cur-Lip on mitochondrial quality control in rBMSCs, we assayed the mRNA expression of mitochondrial biosynthesis gene *PGC-1 α* , mitochondrial dynamics related genes along with the expression of mitophagy related proteins (Fig. 6). RT-qPCR analysis exhibited that D-gal down-regulated the mRNA expression of *PGC-1 α* and mitochondrial fission gene *Drp1* (Fig. 6A, $p < 0.05$). Western blotting results revealed that D-gal decreased the protein levels of PINK1 and LC-3B II/I, and increased p62 expression compared with the control group (Fig. 6B, $p < 0.05$, $p < 0.01$). 10 μ mol/L Cur-Lip treatment significantly upregulated the mRNA level of *Drp1* and *PGC-1 α* compared with the D-gal group (Fig. 6A, $p < 0.05$, $p < 0.01$). However, mitochondrial fusion-related genes (*Mfn1*, *Mfn2*, and *OPA1*) showed no remarkable difference among groups (Fig. 6A). The expressions of LC3B II/I, PINK1, and Parkin proteins were significantly increased, and p62 decreased after the treatment of 10 μ mol/L Cur-Lip compared to the D-gal group (Fig. 6B, $p < 0.05$, $p < 0.01$).

The above results indicated that Cur-Lip could protect mitochondrial function induced by D-gal, improve mitochondrial dynamics and activate mitophagy in rBMSCs.

Cur-lip slowed senescence of rBMSCs involved in activating mitophagy

To further investigate the relationship between the protective role of Cur-Lip in rBMSCs and mitophagy, we used mitophagy inhibitor (Mdivi-1) or activator (Rapa) to modulate mitophagy. The western blotting results suggested that Cur-Lip and Rapa treatment increased PINK1 and Parkin protein expressions compared to the D-gal group (Fig. 7A, $p < 0.05$, $p < 0.01$). Furthermore, the colocalization of mitochondria with lysosomes also increased in the Cur-Lip and Rapa treatment groups (Fig. 7B). The mdivi-1 treatment significantly reversed the effect of Cur-Lip in promoting mitophagy (Fig. 7A, $p < 0.05$, $p < 0.01$).

Compared with the D-gal group, the Cur-Lip and Rapa treatment decreased the ratio of SA- β -gal staining-positive cells (Fig. 8A, $p < 0.05$, $p < 0.01$), exhibited lower mtROS (Fig. 8B, $p < 0.01$), and increased mt $\Delta\psi$ m

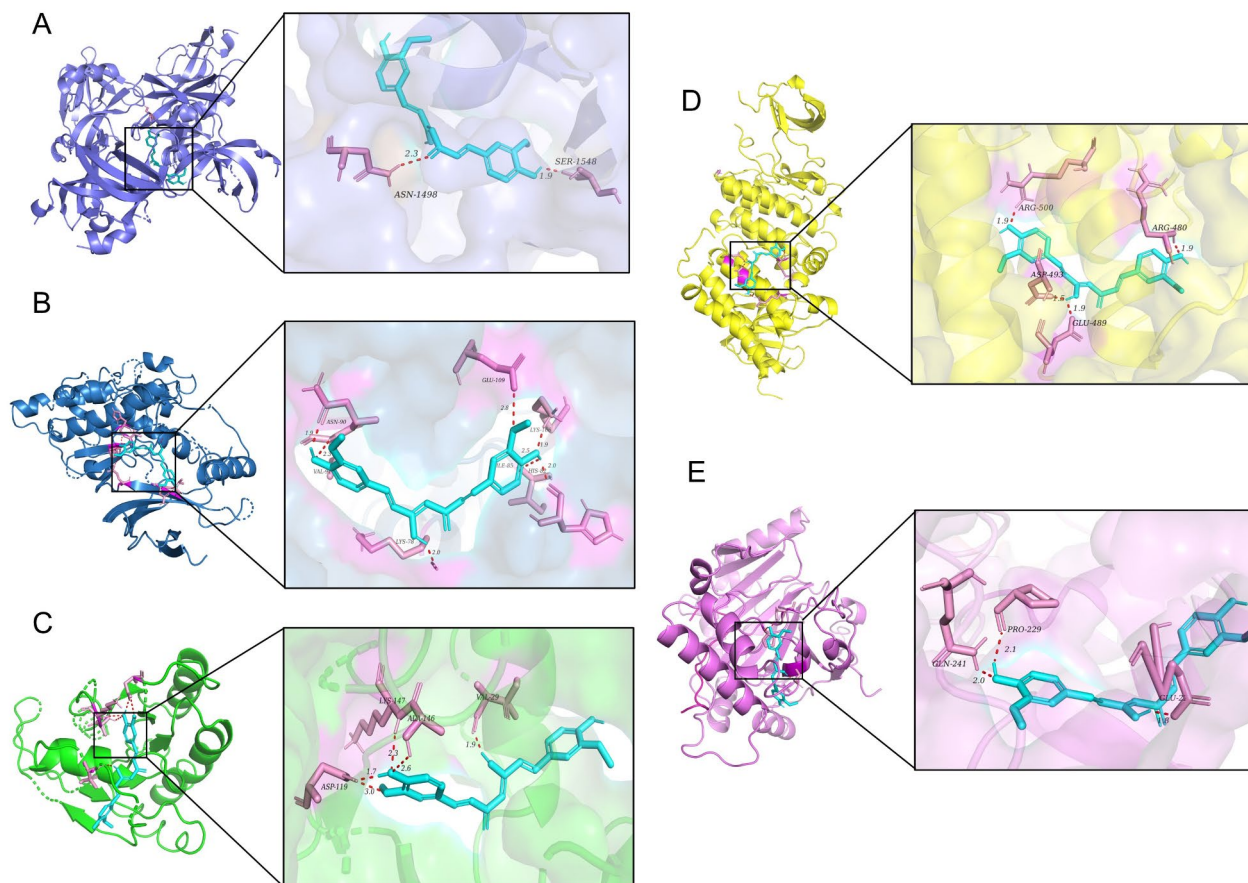


Fig. 2. Molecular docking between Cur and mitophagy-related proteins. **(A)** Cur-TP53. **(B)** Cur-MAPK8. **(C)** Cur-HRAS. **(D)** Cur-SRC. **(E)** Cur-HIF1 α . Dotted line: molecular binding site.

(Fig. 8C, $p < 0.01$). However, the effects of Cur-Lip on mitochondrial function and senescence phenotype of rBMSCs were reversed by mitophagy inhibitor Mdivi-1 (Fig. 8A-C, $p < 0.01$). The above results suggested that Cur-Lip could removal of damaged mitochondria, maintain mitochondrial function and alleviate senescence of rBMSC by activating mitophagy.

Discussion

The senescence of MSCs is inevitably affected by age and diseases, thus limiting MSC therapeutic potential²⁶. Chinese medicinal have multi-target and multi-pathway features, have been suggested to promote longevity and be promising tools for delaying aging²⁷. In this study, we found that Cur-Lip protected mitochondrial function and alleviated the senescence of rBMSCs by activating mitophagy.

Long-term exposure to oxidative stress is a major factor in aging^{28,29}. The anti-aging properties of Cur have been extensively examined, revealing its potential to positively impact aging and age-related ailments at both the cellular and tissue levels. Studies have shown that pre-treatment with Cur can reduce ROS production, protect cells from premature senescence, and promote osteogenesis differentiation of MSCs^{11,30}. The present study showed that Cur-Lip can improve the proliferation of cells, decrease the activity of SA- β -gal, and down-regulate the expression of p53/p21 and p16 proteins in D-gal-induced rBMSCs. Previous studies have found that Cur in the range of 10 $\mu\text{mol/L}$ has a beneficial effect on cBMSCs for 24 h¹⁴, whereas we found that treatment with 5 $\mu\text{mol/L}$ and 10 $\mu\text{mol/L}$ Cur-Lip for 48 h can maintain cell vitality, but Cur-Lip at a concentration of 20 $\mu\text{mol/L}$ or above showed no significant beneficial effect and even had a cytotoxic effect (Supplementary file S4). Another study have found that 7-day-treatment of Cur at a concentration of 25 $\mu\text{mol/L}$ or above significantly attenuated the maintenance of human BM-MSCs, while 10 $\mu\text{mol/L}$ Cur reduced BM-MSC proliferation and hindered their migration with increasing cell apoptosis³¹. Furthermore, Cur combined with nanosphere can improve the stability, bioavailability, and control the release rate. 1ng/mL nanosphere-loaded Cur increased the motility of umbilical cord blood MSCs and the migration efficacy was 10,000 times greater than Cur²¹. Therefore, the safety impact of Cur exposure on MSCs should be carefully considered before implementing different biomedical studies, and more clinical trials are necessary to assess the safety of Cur at different doses, treatment length and forms.

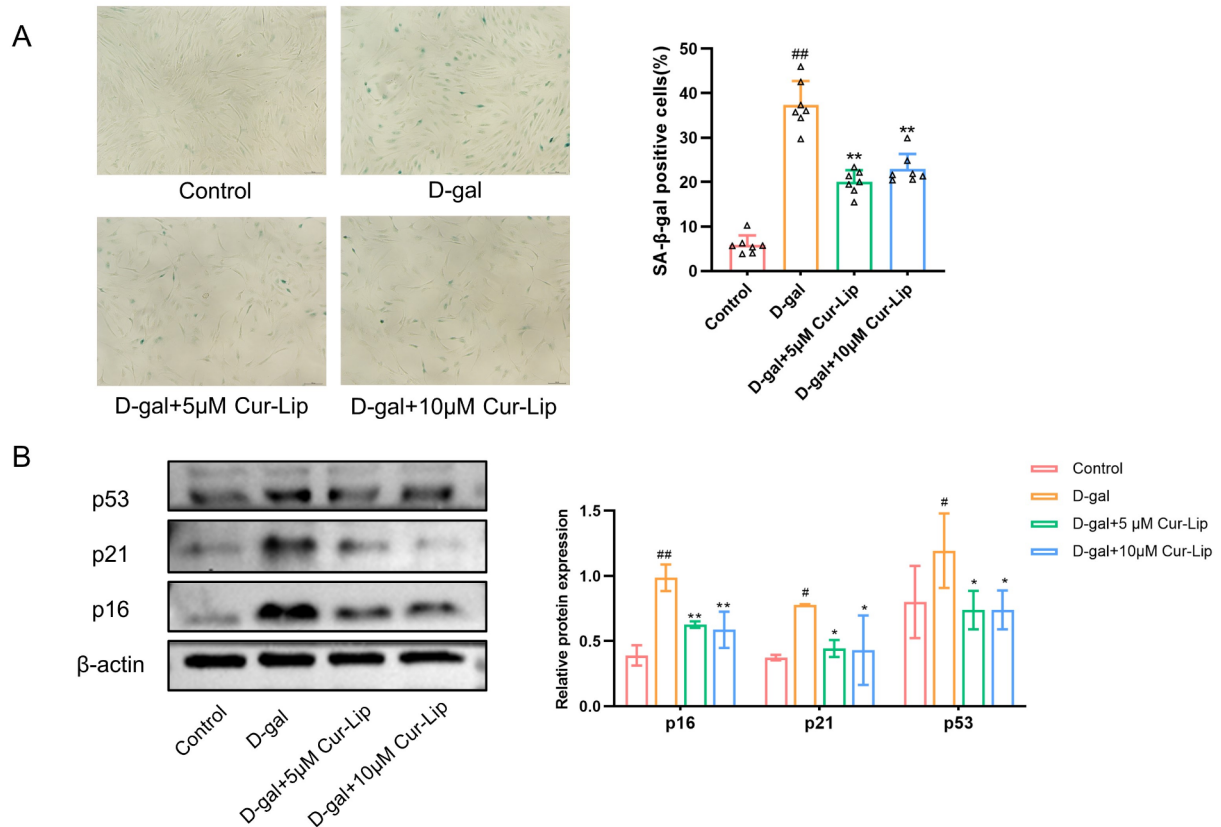


Fig. 3. Cur-Lip alleviated D-gal induced senescence of rBMSCs. (A) SA-β-gal assay in rBMSCs. Scale bar = 150 μm. (B) The effects of Cur-Lip on the protein expression of p16, p21 and p53 in rBMSCs. * $p < 0.05$, ** $p < 0.01$ vs. D-gal group; # $p < 0.05$, ## $p < 0.01$ vs. control group (same as below).

Network pharmacology enables to investigate potential targets and interactions of traditional chinese medicine, and has been used to predict potential mechanisms of Cur in the treatment of degenerative diseases and cancer^{16,32}. In this study, network pharmacology was used to predict the mechanism of Cur effect on the senescence of MSCs. The targets including TP53, MAPK8, SRC, HRAS, and HIF1A were the key targets of Cur effect on the senescence of MSCs, which enriched in the mitophagy pathway. p53 is closely associated with the senescence of MSCs. In senescent MSCs, the expression level of p53 increased, and the regulating mitophagy in MSCs by regulating p53 and parkin expressions had been shown to mitigate stress-induced senescence and apoptosis of MSCs³³. HIF-1 α also regulated mitophagy level to improved aging in mice³⁴. Activated the HIF-1 signaling pathway can promote MSC differentiation and proliferation³⁵. Both the HIF-1 and p53 are involved in the cellular response to hypoxia. HIF-1 can interact with p53 and participate in inducing apoptosis under hypoxia³⁶. KEGG signaling pathways closely related to aging were screened out, such as FOXO signaling pathway, MAPK signaling pathway, PI3K-Akt signaling pathway, Mitophagy and Wnt signaling pathway. The Akt/PI3K pathway plays a crucial role in the aging process. As a downstream component, FOXO1 is involved in regulating various biological activities of MSCs, such as cell proliferation, survival, and osteogenic differentiation^{37,38}. P38/MAPK is an important pathway that transmits signals from the cell membrane to the nucleus and is related to the self-renewal, cell proliferation and differentiation of MSCs³⁹. Recent studies have found that inhibiting Wnt signaling can slow the senescence of BMSCs⁴⁰. To be noted, FOXO, PI3K-Akt, Wnt and HIF-1 signaling are also involved in the regulation of mitophagy^{33,41–44}. This provides a reference for us to study the role of Cur-Lip on the senescence of rBMSCs.

Mitochondria are cellular energy factories and signal transmission centers. When the mitochondrial structure is damaged, it will lead to mitochondria dysfunction including the decrease of mt $\Delta\psi$ m and the increase of ROS production, ultimately exacerbating cellular damage and triggering aging⁴⁵. The potential of Cur in maintaining mitochondrial function has been reported⁴⁶. Studies have shown that treating LLC-PK1 cells with 30 μmol/L Cur for 24 h would lead to an increase in the expression level of PGC-1 α , which participates in a variety of mitochondria-related metabolic pathways and closely related to the mitochondrial biosynthesis process, and attenuated gentamicin-induced kidney mitochondrial dysfunction⁴⁷. Furthermore, mitochondria can preserve their structure and functionality through ongoing dynamic processes of fission and fusion. The process of fission serves to segregate impaired mitochondria from healthy ones, with the damaged portions undergoing mitophagy⁴⁸. In our study, D-gal impaired mitochondrial integrity and function in rBMSCs. Cur-Lip treatment reduced mtROS, increased mt $\Delta\psi$ m, and upregulated the expression of PGC-1 α and the mitochondrial fission

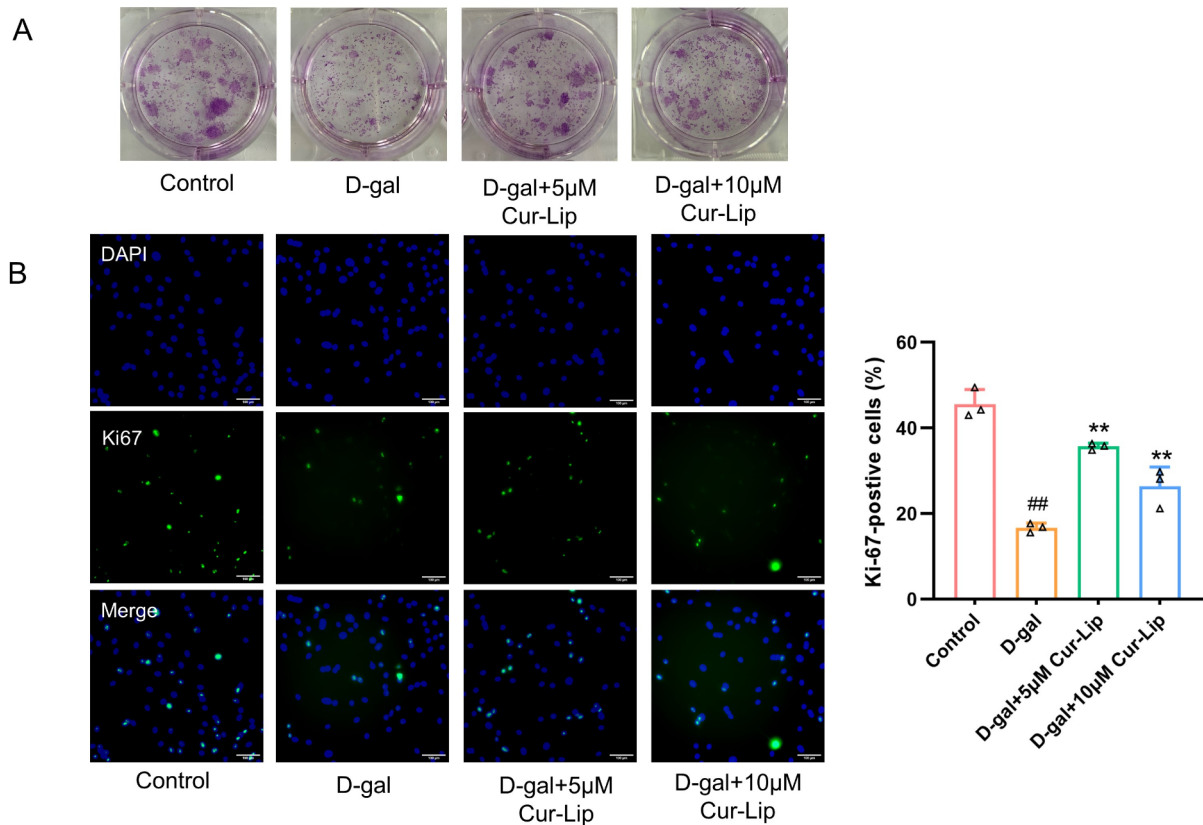


Fig. 4. Cur-Lip improved cell proliferation in senescent rBMSCs. (A) Clone formation assay. (B) Representative images of Ki67 staining in rBMSCs. Scale bar = 100 µm.

gene *Drp1*. Cur-Lip promoted mitochondrial fission in senescence rBMSCs, which might be a prerequisite for mitophagy.

The role of mitophagy in MSCs has attracted extensive attention. Modulating mitophagy in MSCs can counteract stress-induced apoptosis and senescence^{11,49}. The classic mitophagy pathway is initiated by the PINK1-Parkin-dependent pathway, in which PINK1 recruits Parkin and stimulates the activity of E3 ligase under cellular stress conditions, activates Parkin and then ubiquitinates substrate proteins, leading to lysosome-mediated degradation of mitochondria. Notably, upregulation of Parkin in BMSCs has been shown to enhance ubiquitination of mitochondrial outer membrane proteins, and reduce the activity of SA-β-gal, indicating that mitophagy plays a crucial role in regulating senescence of MSCs³³. Studies have shown that Cur can serve as a regulator of mitophagy, maintain mitochondrial homeostasis and ameliorate cellular damage caused by oxidative stress^{16,50}. However, the research of Cur mainly focuses on the regulation of mitophagy in neural cells and tumor cells, and there are limited reports in MSCs^{51,52}. Our study found that 10µmol/L Cur-Lip activated mitophagy by upregulating mitophagy-related proteins (PINK1, Parkin, and LC-3B II/I), decreasing levels of p62 protein, and enhancing the colocalization of mitochondria and lysosomes, which was similar to the effects of mitophagy activator Rapa. Both Cur-Lip and Rapa treatments were effective in mitigating the observed senescence phenotypes. When the mitophagy inhibitor Mdivi-1 was given, these effects of Cur-Lip were significantly reduced or even eliminated, indicating that Cur-Lip indeed alleviates the senescence of rBMSCs by activating mitophagy.

Conclusions

In present study, network pharmacology was applied to predict the targets and mechanisms between Cur and senescence of MSCs. It was then verified via in vitro experiments, showing that Cur-Lip alleviated senescence of rBMSC and improved mitochondrial dysfunction by activating mitophagy. Future studies are recommended to verify this finding in vivo and can focus on the effect of liposomes-curcumin on MSCs via other potential pathways, which is of great significance for preventing aging and treating aging-related diseases.

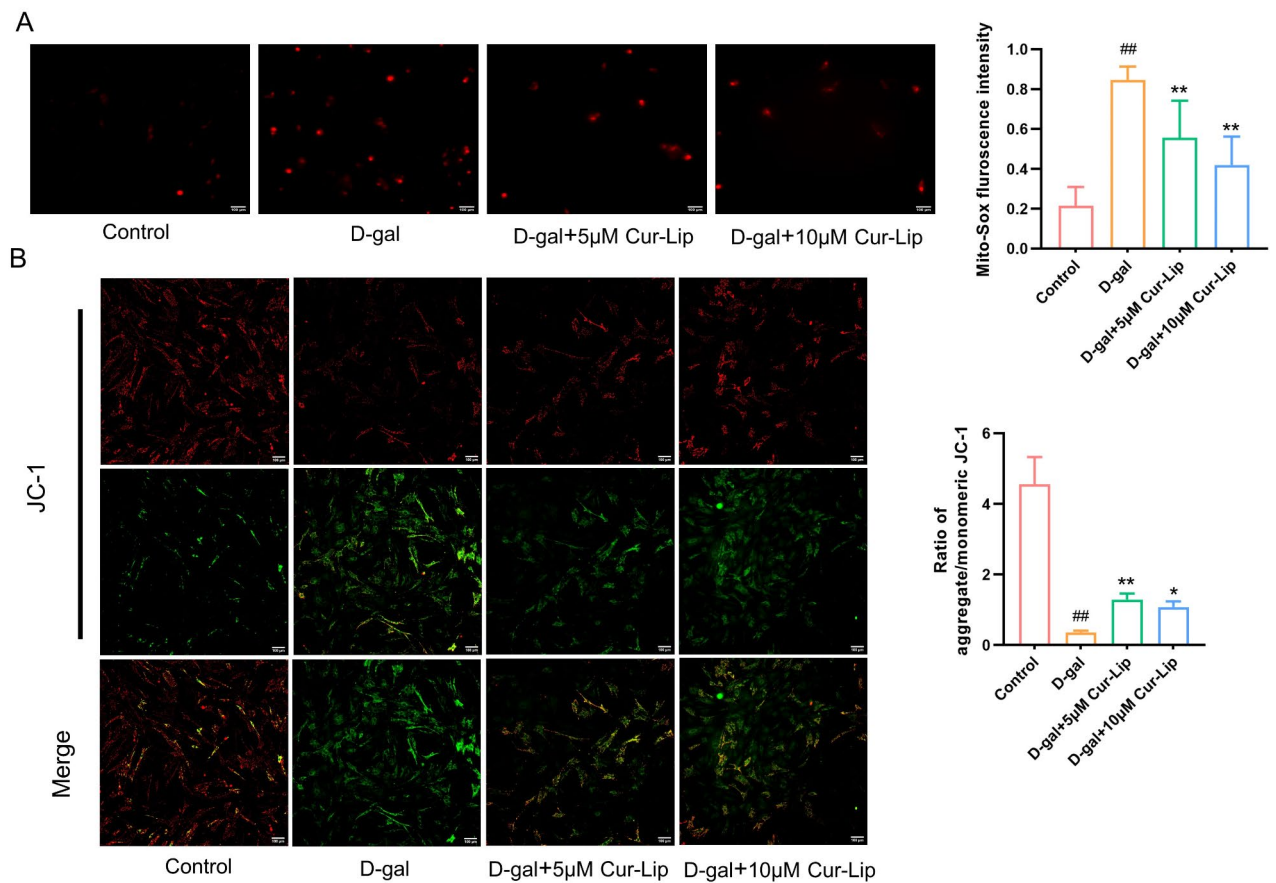
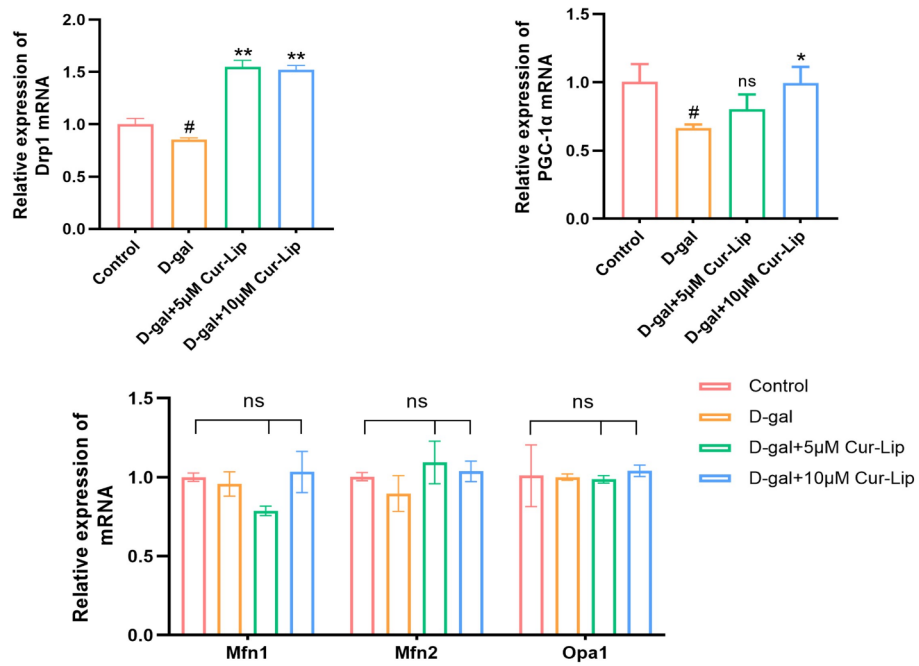


Fig. 5. The protective effect of Cur-Lip on mitochondrial function in rBMSCs. **(A)** Mitochondrial ROS generation. Scale bar = 100 μ m. **(B)** Mitochondrial membrane potential. Scale bar = 100 μ m.

A



B

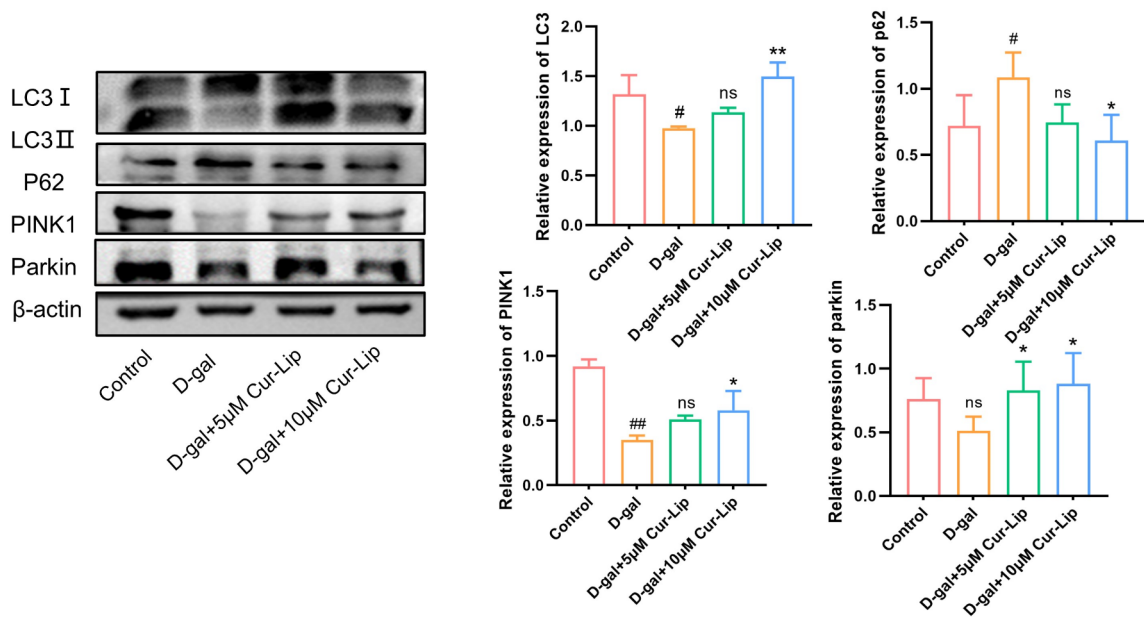


Fig. 6. Cur-Lip promoted mitochondrial quality control in rBMSCs. (A) The mRNA expression of *Opa1*, *Mfn1*, *Mfn2*, *Drp1* and *PGC-1α* in rBMSCs. (B) Cur-Lip increased the expression levels of mitophagy-related proteins in rBMSCs.

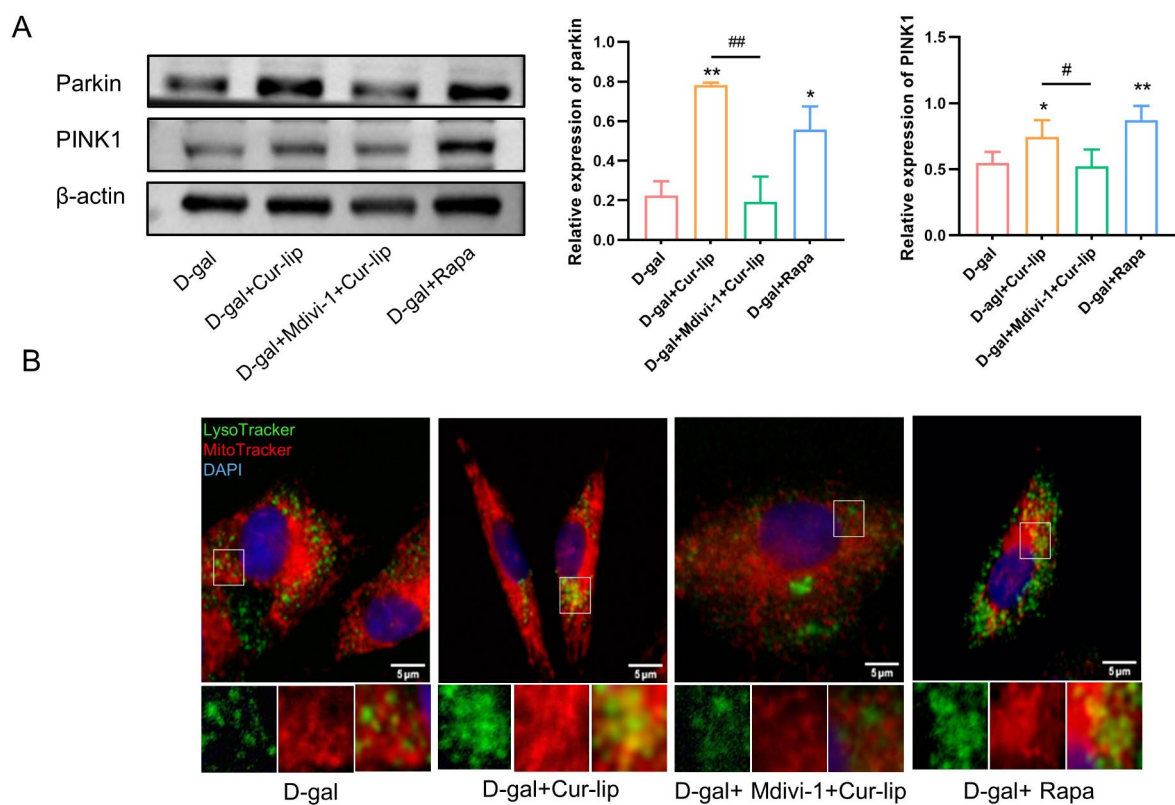


Fig. 7. The level of mitophagy after treatment with each group. **(A)** Expression levels of mitophagy-specific proteins PINK1 and Parkin. **(B)** Co-localization assay in rBMSCs with Lyso-Tracker (green) and Mito-Tracker (Red). Blue staining = DAPI. Scale bars = 5 μm . * $p < 0.05$, ** $p < 0.01$ vs. D-gal group; # $p < 0.05$, ## $p < 0.01$ vs Cur-Lip group (same as below).

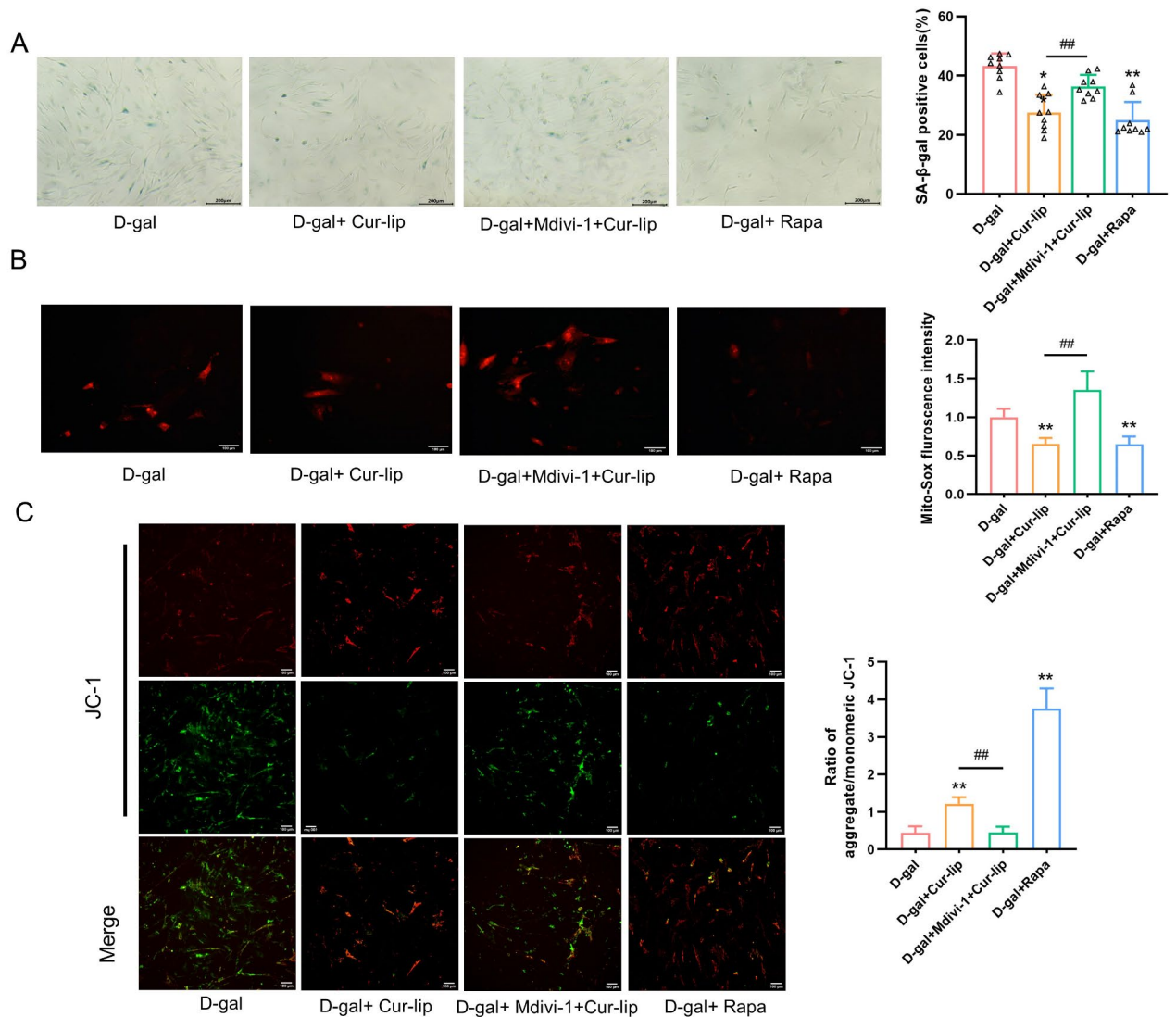


Fig. 8. Mitophagy inhibited the senescence of rBMSCs. (A) SA-β-gal assay in rBMSCs. Scale bars = 200 μm. (B) Mitochondrial ROS generation. Scale bars = 100 μm. (C) Mitochondrial membrane potential.

Data availability

The authors confirm that all data underlying the findings are fully available and can be obtained after submitting a request to the corresponding author.

Received: 4 June 2024; Accepted: 6 December 2024

Published online: 28 December 2024

References

1. Fitzsimmons, R., Mazurek, M. S., Soos, A. & Simmons, C. A. Mesenchymal stromal/stem cells in regenerative medicine and tissue engineering. *Stem Cells Int.* **2018**, 8031718–8031733 (2018).
2. Zhu, Y., Ge, J., Huang, C., Liu, H. & Jiang, H. Application of mesenchymal stem cell therapy for aging Frailty: From mechanisms to therapeutics. *Theranostics* **11**, 5675–5685 (2021).
3. Chen, H., Liu, O., Chen, S. & Zhou, Y. Aging and mesenchymal stem cells: Therapeutic opportunities and challenges in the Older Group. *Gerontology* **68**, 339–352 (2022).
4. Abruzzo, P. M. et al. Herb-derived products: Natural tools to delay and counteract stem cell senescence. *Stem Cells Int.* **2020**, 8827038–8827064 (2020).
5. Vono, R., Jover, G. E., Spinetti, G. & Madeddu, P. Oxidative stress in mesenchymal stem cell senescence: Regulation by coding and noncoding Rnas. *Antioxid. Redox Signal.* **29**, 864–879 (2018).
6. Denu, R. A. & Hematti, P. Effects of oxidative stress on mesenchymal stem cell biology. *Oxidative Med. Cell. Longev.* **2016**, 2989076–2989085 (2016).
7. Pernas, L., Scorrano, L. Mito-morphosis: Mitochondrial fusion, fission, and cristae remodeling as key mediators of cellular function. *Annu. Rev. Physiol.* **78**, 505–531 (2016).
8. Liu, L. et al. Mitophagy and its contribution to metabolic and aging-associated disorders. *Antioxid. Redox Signal.* **32**, 906–927 (2020).

9. Pickles, S., Vigié, P. & Youle, R. J. Mitophagy and quality control mechanisms in mitochondrial maintenance. *Curr. Biol.* **28**, R170–R185 (2018).
10. Naik, P. P., Birbrair, A. & Bhutia, S. K. Mitophagy-driven metabolic switch reprograms stem cell fate. *Cell. Mol. Life Sci.* **76**, 27–43 (2019).
11. Feng, X., Yin, W., Wang, J., Feng, L. & Kang, Y. J. Mitophagy promotes the stemness of bone marrow-derived mesenchymal stem cells. *Exp. Biol. Med.* **246**, 97–105 (2021).
12. Patel, S. S. et al. Cellular and molecular mechanisms of curcumin in prevention and treatment of disease. *Crit. Rev. Food Sci. Nutr.* **60**, 887–939 (2020).
13. Zia, A., Farkhondeh, T., Pourbagher-Shahri, A. M. & Samarghandian, S. The role of curcumin in aging and senescence: Molecular mechanisms. *Biomed. Pharmacother.* **134**, 111119–111128 (2021).
14. Deng, J. et al. Curcumin alleviates the senescence of canine bone marrow mesenchymal stem cells during in vitro expansion by activating the autophagy pathway. *Int. J. Mol. Sci.* **22**, 11356–11376 (2021).
15. Ortega-Dominguez, B. et al. Curcumin prevents Cisplatin-Induced renal alterations in mitochondrial bioenergetics and dynamic. *Food Chem. Toxicol.* **107**, 373–385 (2017).
16. Jin, Z. et al. Curcumin exerts chondroprotective effects against osteoarthritis by promoting Ampk/Pink1/Parkin-mediated mitophagy. *Biomed. Pharmacother.* **151**, 113092–113102 (2022).
17. Lone, J., Choi, J. H., Kim, S. W. & Yun, J. W. Curcumin induces Brown Fat-Like phenotype in 3T3-L1 and primary White adipocytes. *J. Nutr. Biochem.* **27**, 193–202 (2016).
18. Mahjoob, M. & Stochaj, U. Curcumin nanoformulations to combat aging-related diseases. *Ageing Res. Rev.* **69**, 101364 (2021).
19. Huang, M. et al. Liposome co-encapsulation as a strategy for the delivery of curcumin and resveratrol. *Food Funct.* **10**, 6447–6458 (2019).
20. Chen, Y., Lu, Y., Lee, R. J. & Xiang, G. Nano encapsulated curcumin: And its potential for biomedical applications. *Int. J. Nanomed.* **15**, 3099–3120 (2020).
21. Kim, D. W., Choi, C. H., Park, J. P. & Lee, S. J. Nanospheres loaded with Curcumin improve the Bioactivity of umbilical cord blood-mesenchymal stem cells Via C-Src activation during the skin wound healing process. *Cells* **9**, 1467–1485 (2020).
22. Nogales, C. et al. Network pharmacology: Curing causal mechanisms instead of treating symptoms. *Trends Pharmacol. Sci.* **43**, 136–150 (2022).
23. Li, X. et al. Network pharmacology approaches for research of traditional Chinese medicines. *Chin. J. Nat. Med.* **21**, 323–332 (2023).
24. Zhang, D. et al. Autophagy inhibits the mesenchymal stem cell aging induced by D-Galactose through Ros/Jnk/P38 signalling. *Clin. Exp. Pharmacol. Physiol.* **47**, 466–477 (2020).
25. Kanehisa, M. & Goto, S. KEGG: Kyoto encyclopedia of genes and genomes. *Nucleic Acids Res.* **28**, 27–30 (2000).
26. Liu, J., Ding, Y., Liu, Z. & Liang, X. Senescence in mesenchymal stem cells: Functional alterations, molecular mechanisms, and rejuvenation strategies. *Front. Cell. Dev. Biol.* **8**, 258–274 (2020).
27. Gao, L. et al. Antiaging effects of Dietary supplements and natural products. *Front. Pharmacol.* **14**, 1192714–1192733 (2023).
28. Ye, G. et al. Oxidative stress-mediated mitochondrial dysfunction facilitates mesenchymal stem cell senescence in Ankylosing Spondylitis. *Cell. Death Dis.* **11**, 775–787 (2020).
29. Denu, R. A. & Hematti, P. Optimization of oxidative stress for mesenchymal Stromal/Stem cell engraftment, function and longevity. *Free Radic Biol. Med.* **167**, 193–200 (2021).
30. Nir, D. et al. Antioxidants attenuate heat shock induced premature senescence of bovine mesenchymal stem cells. *Int. J. Mol. Sci.* **23**, 5750–5765 (2022).
31. Yang, Q., Leong, S. A., Chan, K. P., Yuan, X. L. & Ng, T. K. Complex effect of continuous curcumin exposure on human bone marrow-derived mesenchymal stem cell regenerative properties through Matrix Metalloproteinase Regulation. *Basic. Clin. Pharmacol. Toxicol.* **128**, 141–153 (2021).
32. He, Q. et al. Exploring the mechanism of curcumin in the treatment of colon cancer based on network pharmacology and molecular docking. *Front. Pharmacol.* **14**, 1102581–1102596 (2023).
33. Zhang, F. et al. P53 and Parkin co-regulate mitophagy in bone marrow mesenchymal stem cells to promote the repair of early steroid-induced osteonecrosis of the femoral head. *Cell. Death Dis.* **11**, 42–57 (2020).
34. Gao, T., Li, Y., Wang, X. & Ren, F. Alginate oligosaccharide-mediated butyrate-Hif-1Alpha Axis improves skin aging in mice. *J. Pharm. Anal.* **14**, 100911–100925 (2024).
35. Chen, X. et al. Ginsenoside Ck cooperates with bone mesenchymal stem cells to enhance angiogenesis post-stroke via Glut1 and Hif-1Alpha/Vegf pathway. *Phytother Res.* **38**, 4321–4335 (2024).
36. Zhou, C. H., Zhang, X. P., Liu, F. & Wang, W. Modeling the interplay between the Hif-1 and P53 pathways in Hypoxia. *Sci. Rep.* **5**, 13834–13843 (2015).
37. Baker, N., Sohn, J. & Tuan, R. S. Promotion of human mesenchymal stem cell osteogenesis by Pi3-Kinase/Akt signaling, and the influence of Caveolin-1/Cholesterol homeostasis. *Stem Cell. Res. Ther.* **6**, 238–248 (2015).
38. Suwanmanee, G., Tantrawatpan, C., Kheolamai, P., Paraoan, L. & Manochantr, S. Fucoxanthin diminishes oxidative stress damage in human placenta-derived mesenchymal stem cells through the Pi3K/Akt/Nrf-2 pathway. *Sci. Rep.* **13**, 22974–22993 (2023).
39. Budgude, P., Kale, V. & Vaidya, A. Pharmacological inhibition of P38 Mapk rejuvenates bone marrow derived-mesenchymal stromal cells and boosts their hematopoietic stem cell-supportive ability. *Stem Cell. Rev. Rep.* **17**, 2210–2222 (2021).
40. Kang, X. et al. Zuogui Wan slowed senescence of bone marrow mesenchymal stem cells by suppressing Wnt/Beta-Catenin signaling. *J. Ethnopharmacol.* **294**, 115323–115334 (2022).
41. Fu, Z. J. et al. Hif-1Alpha-Bnip3-mediated mitophagy in tubular cells protects against renal Ischemia/Reperfusion Injury. *Redox Biol.* **36**, 101671–101686 (2020).
42. Liu, B. et al. Zhen-Wu-Tang Induced Mitophagy to protect mitochondrial function in chronic glomerulonephritis Via Pi3K/Akt/Mtor and Ampk pathways. *Front. Pharmacol.* **12**, 777670–777682 (2021).
43. Yao, J. et al. Cdk9 inhibition blocks the initiation of Pink1-Prkn-mediated mitophagy by regulating the Sirt1-Foxo3-Bnip3 axis and enhances the therapeutic effects involving mitochondrial dysfunction in hepatocellular carcinoma. *Autophagy* **18**, 1879–1897 (2022).
44. Liu, L. J., Lv, Z., Xue, X., Xing, Z. Y. & Zhu, F. Canonical wnt signaling activated by Wnt7B contributes to L-Hbs-mediated Sorafenib resistance in hepatocellular carcinoma by inhibiting mitophagy. *Cancers* **14**, 5781–5797 (2022).
45. Miwa, S., Kashyap, S., Chini, E. & von Zglinicki, T. Mitochondrial dysfunction in cell senescence and aging. *J. Clin. Invest.* **132**, e158447–e158455 (2022).
46. Banji, O. J., Banji, D. & Ch, K. Curcumin and hesperidin improve cognition by suppressing mitochondrial dysfunction and apoptosis induced by D-Galactose in rat brain. *Food Chem. Toxicol.* **74**, 51–59 (2014).
47. Negrette-Guzman, M. et al. Curcumin attenuates gentamicin-induced kidney mitochondrial alterations: Possible role of a mitochondrial biogenesis mechanism. *Evid.-Based Complement Altern. Med.* **2015**, 917435–917451 (2015)
48. Ren, L. et al. Mitochondrial dynamics: Fission and fusion in fate determination of mesenchymal stem cells. *Front. Cell. Dev. Biol.* **8**, 580070–580087 (2020).
49. Liu, F. et al. Lrrc17 controls Bmsc senescence via mitophagy and inhibits the therapeutic effect of Bmscs on ovariectomy-induced bone loss. *Redox Biol.* **43**, 101963–101976 (2021).

50. Cao, S. et al. Curcumin ameliorates oxidative stress-induced intestinal barrier injury and mitochondrial damage by promoting parkin dependent mitophagy through Ampk-Tfeb signal pathway. *Free Radic Biol. Med.* **147**, 8–22 (2020).
51. WANG, X., LUO, L. E. U. N. G. A. W., XU, C. & J. & Tem Observation of Ultrasound-Induced Mitophagy in Nasopharyngeal Carcinoma Cells in the Presence of Curcumin. *Exp. Ther. Med.* **3**, 146–148 (2012).
52. Wang, W. & Xu, J. Curcumin attenuates cerebral ischemia-reperfusion Injury through regulating mitophagy and preserving mitochondrial function. *Curr. Neurovasc Res.* **17**, 113–122 (2020).

Acknowledgements

This research was supported by Southwest Medical University-level research project, grant number (2021ZKMS033). The authors appreciate to the Experimental Animal Centre of Southwest Medical University, Luzhou, China.

Author contributions

W.L., L.F. Investigation. W.L. Writing—original draft. Y.H. Methodology and writing—review and editing. D.Y., K.Z. Provide experimental materials. L.S., S.C. Supervision and project administration. C.G., S.Y. Conceptualization and study Supervision. Conceptualization, Methodology, Resources. All authors have read and agreed to the published version of the manuscript.

Declarations

Competing interests

The authors declare no competing interests.

Ethical approval

The study was approved by the Ethics Committee of the institutional Animal Care and Use Committee of Southwest Medical University (Approval No. swmu20230085).

Additional information

Supplementary Information The online version contains supplementary material available at <https://doi.org/10.1038/s41598-024-82614-1>.

Correspondence and requests for materials should be addressed to C.G. or S.Y.

Reprints and permissions information is available at www.nature.com/reprints.

Publisher's note Springer Nature remains neutral with regard to jurisdictional claims in published maps and institutional affiliations.

Open Access This article is licensed under a Creative Commons Attribution-NonCommercial-NoDerivatives 4.0 International License, which permits any non-commercial use, sharing, distribution and reproduction in any medium or format, as long as you give appropriate credit to the original author(s) and the source, provide a link to the Creative Commons licence, and indicate if you modified the licensed material. You do not have permission under this licence to share adapted material derived from this article or parts of it. The images or other third party material in this article are included in the article's Creative Commons licence, unless indicated otherwise in a credit line to the material. If material is not included in the article's Creative Commons licence and your intended use is not permitted by statutory regulation or exceeds the permitted use, you will need to obtain permission directly from the copyright holder. To view a copy of this licence, visit <http://creativecommons.org/licenses/by-nc-nd/4.0/>.

© The Author(s) 2024